Biological Structure and Dynamics, ISBN 0-940030-46-2
Proceedings of the Ninth Conversation, State University of New York. Albany, NY 1995
Eds. Ramaswamy H. Sarma and Mukti H. Sarma, ©Adenine Press 1996

The Combination of Functional, Genetic, Biochemical, Microscopical and Crystallographic Studies Led to Initial Phasing of Data Collected from Ribosomal Crystals at Intermediate Resolution

F. Franceschi[1]*, S. Weinstein[2], I. Sagi[2,3], M. Peretz[2], V. Weinrich[2], S. Morlang[1], K. Anagnostopoulos[1], N. Böddeker[1], M. Geva[2], I. Levin[2], I. Agmon[2], Z. Berkovitch-Yellin[2,3], T. Choli[4], P. Tsiboli[4], F. Schlünzen[3], H.A.S. Hansen[3], H. Bartels[3], W.S. Bennett[3], N. Volkmann[3], J. Thygesen[3], J. Harms[3], A. Zaytzev-Bashan[2], S. Krumbholz[3], R. Sharon[2], A. Dribin[2], E. Maltz[2] and A. Yonath[2,3]

[1] Max-Planck-Inst. for Molecular Genetics, Ihnestr. 73, 14195 Berlin, Germany

[2] Department of Structural Biology, Weizmann Institute of Sciences, Rehovot 76100, Israel

[3] Max-Planck-Lab. for Ribosomal Structure c/o DESY, Notkestr. 85, 22603 Hamburg, Germany

[4] Lab. of Biochem. Dept. Chemistry, Aristotle Univ. of Thessaloniki, 54006 Thessaloniki, Greece

Abstract

The application of a multi-directional approach, combining functional, biochemical, genetic and organometallic procedures together with X-ray, neutron and electron diffraction methods led to initial phasing of data collected from ribosomal crystals, using the isomorphous replacement as well as ab-initio methods. Consequently, preliminary electron density maps of the large and the small

Abbreviations: 70S, 30S, 50S: the commonly used names for bacterial ribosomes and their small and large subunits, respectively, given according to their sedimentation coefficients. E, B, T, and H in front of these names or the number of a ribosomal protein show the bacterial source (*Escherichia coli*; *Bacillus stearothermophilus*, *Thermus thermophilus* and *Haloarcula marismortui*, respectively). rRNA and r-proteins: ribosomal RNA and ribosomal proteins. For proteins: L shows that the protein is of the large (50S) subunit, and S of the small (30S) one (e.g. BL11 is protein 11 in the large ribosomal subunit from *B. stearothermophilus*). The symbol HmaL# indicates that this particular protein (of *H. marismortui*) is homologous to protein # from *E. coli*; MIR, SIR: the multiple and single isomorphous phasing methods.

*Author to whom correspondence should be sent. Phone: 49-30-84131222; Fax: 49-30-84131380; E-mail: Franceschi@mpimg-berlin-dahlem.mpg.de

ribosomal particles from halophilic and thermophilic bacteria have been constructed at intermediate resolution. These maps contain features comparable in size to what is expected for the corresponding particles, and their packing arrangements are in accord with the motifs observed in thin sections of the crystals by electron microscopy.

For phasing the crystallographic data at higher resolution, procedures are being developed for specific and quantitative derivatization of the ribosomal particles at selected locations with rather small and dense heavy atom clusters. Potential binding sites are being inserted either by site directed mutagenesis or by chemical modifications at exposed positions on the surface of the particles which give rise to the highest resolution obtained so far for ribosomal crystals, namely H50S and T30S which diffract to 2.9 Å and 7.3 Å, respectively. The choice of the appropriates sites for cluster binding is based on information obtained from sequence studies and from surface characterization by enzymatic and chemical methods. To facilitate quantitative and specific binding, procedures are developed for the detachment of selected ribosomal proteins and for their incorporation into core particles. The genes of these proteins are being cloned, mutated to introduce cysteines into predetermined sites, and overexpressed.

Two in situ small and stable complexes were isolated from the halophilic ribosome. Aiming at their crystallization and possible modifications, procedures for their production in large quantities are currently being developed.

Initial efforts at low resolution phasing of the X-ray amplitudes by computational procedures were aided by models, reconstructed at low resolution from crystalline arrays of ribosomes and their large subunits. These models have been provisionally interpreted in functional terms. These stimulated the design and the crystallization of complexes mimicking defined functional states, which were found to be of a higher quality than that obtained for isolated ribosomes. They also inspired modeling experiments according to results of functional studies, performed elsewhere, focusing on the progression of nascent proteins.

Introduction

The translation of the genetic code into proteins chains is a fundamental cellular process, mediated in all living cells by an organelle called the ribosome. This is a giant ribonucle-

Table I
Characterized three-dimensional crystal of ribosomal particles.

Source	Grown Form	Cell Dimensions (A)	Resolution (Å)
T70S	MPD *	524x524x306; $P4_12_12$	app. 20
T70S$^{(complex)}$ #	MPD	524x524x306; $P4_12_12$	12
T30S	MPD	407x407x170; $P42_12$	7.3
H50S <	PEG *	210x300x581; $C222_1$	2.9
T50S	AS *	495x495x196; $P4_12_12$	8.7
B50S ^	A *	360x680x920; $P2_12_12$	app. 18
B50S ^<	PEG	308x562x395; 114°; C2	11

*MPD, PEG, AS, A= crystals grown by vapor diffusion in hanginh drops from solutions containing methyl-pentane-diol, polyetheneglycol, ammonium sulphate or low molecular weight alcohols, respectively.
#A complex of 70S ribosomes, 2 molecules phe-tRNA^{phe} and an oligomer of 35 uridines (as mRNA).
^Same for crystals of mutated 50S (lacking protein BL11) and of 50S bound to undecagoldcluster.
<Same for crystal of a complex of 50S+tRNA+a segment (18-20 mers) of a nascent protein chain.

oprotein particle, operating as a giant multi-functional enzyme. A typical bacterial ribosome contains more than quarter of a million atoms and is of a molecular weight of 2.3 million daltons with a sedimentation coefficient of 70S. It is built of two independent subunits of unequal size which associate upon the initiation of protein biosynthesis (50S of 1.45, and 30S of 0.85 million daltons, respectively). About a third of the ribosomal mass comprises some 58-73 different proteins, depending on the source. The rest are 3 chains of rRNA, of a total of about 4500 nucleotides.

To shed light on the molecular mechanisms involved in protein biosynthesis, crystallographic analysis of the three-dimensional structure of the ribosome is being carried out, using crystals of intact ribosomal particles from halophilic and thermophilic bacteria, the only sources which led crystals suitable for crystallographic analysis (TABLE I). Two of these crystal forms diffract to reasonable resolution. Those of the large ribosomal subunits of *H. marismortui*, to 2.9 Å resolution (1) and those of the small subunits of *Thermus thermophilus*, to 7.3 Å resolution (2). The crystallized systems include 70S ribosomes and their complexes mimicking defined functional states, as well as natural, modified and mutated ribosomal subunits (3). Crystallographic data are being collected at cryo temperature from shock frozen crystals with bright synchrotron radiation. As a result of continuous refinement of the crystal growth conditions and the instrumentation and parameters of the data collection, the current crystallographic data are of reasonable quality, which in many cases is comparable to those obtained from crystalline proteins of average size.
In this manuscript we present an overview of our multi-directional efforts, highlighting (a) our latest results in the genetic, biochemical and functional characterization of the halophilic and thermophilic ribosomes, and (b) the construction of the preliminary electron density maps of the small and the large subunits, phased by experimental crystallographic methods and supported by ab-initio procedures. We describe our plans towards the construction of electron density maps for the ribosome and its functional complexes and for extending the level of detail of the current maps. The various strategies expected to be taken for the interpretation of the maps are also being discussed.

Preliminary Isomorphous Replacement Phasing Using Covalently Bound Heavy Atom Derivatives

The assignment of phases to the observed structure factor amplitude is the most crucial, albeit most complicated and unpredictable step in structure determination, even for average-size single proteins or their simple complexes. Clearly, for ribosomal crystals, the magnitude and the complexity of this step is greatly enhanced. Therefore, a multi directional algorithm has been designed, according to which the commonly used phasing techniques in biological crystallography are being employed side by side with efforts at very low resolution phasing by pure computational and semi experimental procedures.

The most productive method for the determination of the phases of unknown structures of macromolecules is *isomorphous replacement.* It is based on the changes in the structure factor amplitudes which are caused by the addition of heavy atoms to the native crystals. Successful derivatization requires attachment of heavy atoms at a limited number of sites within the unit cell, while keeping the crystal structure isomorphous to that of the native

molecule. When only one derivative is available, the Single Isomorphous Replacement (SIR) procedure, which yields ambiguous phasing, is used. When more than one such derivative can be obtained, MIR (multiple isomorphous replacement) is being employed.

The added compounds are chosen according to their potential ability to induce measurable signals, since the differences in the intensities of the reflections of the native and derivatized crystals are being exploited for phasing. Useful heavy atom derivatives for proteins of average size consist of one or two heavy-metal atoms. Because of the large size of the ribosome, ideal compounds for derivatization are compact and dense materials of a proportionally larger number of electrons. Therefore, dense metal clusters, such as undecagold (4), or multi-metal salts, such as polyheteroanions and coordination compounds (TABLE II), are being exploited for the derivatization of ribosomal crystals.

An experiment, aimed at testing the feasibility of phasing the X-ray crystallographic data collected from ribosomal crystals to which a heavy atom cluster has been attached covalently prior to the crystallization led to the construction of SIR electron density map of B50S at 26 Å (5). This approach was chosen although it requires sophisticated synthetic techniques and time-consuming purification procedures, because it maximizes the chances of obtaining a unique derivative with full occupancy.

The B50S particles were chosen for this test, although they are crystallographically the weakest, producing crystals that are unstable, packed with a very low symmetry and diffract to low resolution (6). Nevertheless, their biochemistry and genetics are rather well characterized. These particles possess an exposed -SH group on a protein which is readily detached from the ribosome (BL11), and a mutant, lacking this protein could be obtained by the addition of the antibiotic thiostrepton to the bacterial growth medium.

A monofunctional reagent was prepared from an undecagold cluster, composed of a core of densely packed Au atoms linked directly to each other (4). The core of the undecagold cluster is about 8.2 Å in diameter (4). Therefore it can be treated as a single scattering group at low to medium resolution. This reagent was bound to isolated protein BL11, exploiting its only cysteine. Remarkably, although the binding of the cluster was carried out under denaturing conditions, and although the molecular weight of the undecagold cluster (6200 Da) approaches half of that of the protein (15500 Da), after renaturation, the cluster-bound protein was incorporated into cores lacking this protein, yielding fully derivatized particles.

Table II
Heavy atom compounds used for soaking.

TAMM = tetrakis (acetoxymercuri)-methane)
$(NH_4)_6(P_2W_{18}O_{62})14H_2O$
$K_{14}NaP_5W_{30}O_{110}$
$(K_5O_2)_3(PW_{12}O_{40})$
$Na_{16}((O_3PCH_2PO_3)_4W_{12}O_{36})nH_2O$
$Cs_7(P_2W_{17}O_{61}Co(NC_5H_5))nH_2O$
$K_5H_4((phSn)_3(P_2W_{15}O_{59}))nH_2O$ (ph=phenyl)
$K_5H_4((buSn)_3(P_2W_{15}O_{59}))nH_2O$ (bu=butyl)
$K_7((buSn)_3(P_2W_{17}O_{61}))nH_2O$
$K_{11}H((buSnOH)_3(PW_9O_{34}))nH_2O$
$K_4H_3((buSn)_3(alfaSiW_9O_{31})_2)nH_2O$
$Cs_9H_6((buSnO)_3(alfaSiW_9O_{31})_2)nH_2O$
$Ta_6Br_{12}Cl_2.8H_20$
$Ta_6Br_{14}.8H_20$

Because of the significant lack of isomorphism and the nonuniform mosaic spread, a few data sets had to be collected before a sufficiently isomorphous couple was

detected. Some of these sets contain reflections to 11-15 Å resolution, however meaningful differences were obtained only at lower resolution. After resolving the SIR phase ambiguity by solvent flattening, the 26 Å electron density map shows packing arrangement consistent with the non-crystallographic symmetry found by the self rotation function as well as with the motif observed in electron micrographs of thin sections of these crystals (Fig. 1).

Specific Labeling of Halophilic and Thermophilic Ribosomes

Specific derivatization at predetermined sites on selected ribosomal components may have a considerable value not only in phasing the crystallographic data, but also in the localization of the sites to which the heavy atoms are bound. Such information may be indispensable for the interpretation of high resolution electron density maps. The studies per-

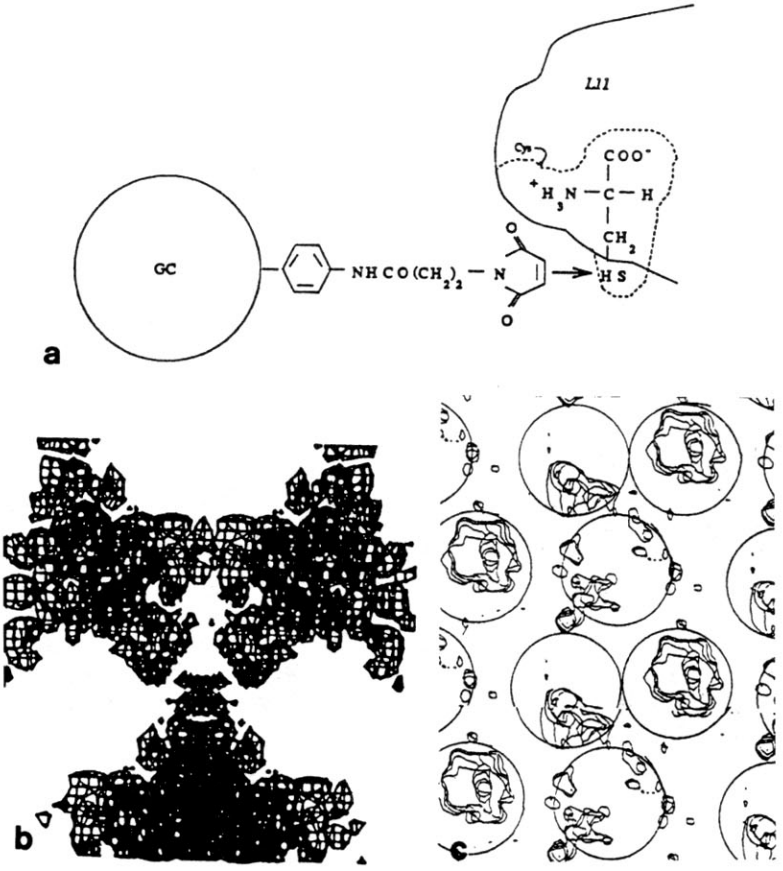

Figure 1:
(a) A schematic representation of the monofunctional reagent of the undecagold cluster bound to the SH group of protein BL11 (5).
(b) The electron density map of B50S after two cycles of solvent flattening assuming 61% solvent, combined with phase combination. The whole unit cell, down the z direction, is shown. Resolution range = 26-60 Å, figure of Merit = 0.71 (5).
(c) A section of 40 Å thickness through the map shown in (b), depicted are the features which can be interpreted as part of the 50S particle, keeping the 3-fold non-crystallographic symmetry.

formed with the undecagold cluster established that phase information can be obtained from bound heavy metal clusters, even when the crystals under investigation are unstable and weakly diffracting and encouraged further effort at the construction of specifically derivatized crystals from the ribosomal particles which diffract to higher resolution, namely H50S and T30S. Assuming the correctness of the preliminary intermediate resolution electron density maps (Figs. 2 and 3) of these two particles, which were phased by soaking crystals in solutions containing heavy atom clusters (7), low resolution phasing by labeling with the large undecagold cluster may be obsolete. Therefore this procedure is currently being extended to the binding of smaller dense clusters, such as TAMM (Table I) or a tetrairidium cluster (8). As these clusters are significantly lighter than the undecagold cluster, for obtaining measurable signals, procedures are being developed for their binding in multiple sites.

It was found that a straight forward extension of the procedures developed for B50S to H50S and T30S was not possible, as there are no naturally exposed sulfhydryls on the surfaces of these particles suitable for derivatization with the undecagold cluster. In addition, because of the significant resistance of the halophilic ribosomes to mutagenesis no protein-depleted core particles could be produced by growing the bacteria on medium containing antibiotics. Also, the chemical methods used for quantitative detachment of selected *E. coli* ribosomal proteins were found unsuitable for the halophilic systems. Furthermore, in contrast to the ease of the incorporation of the gold-cluster bound protein BL11 into depleted cores of *B. stearothermophilus*, protein HmaL11, the halophilic homologue of BL11 (9), can be reconstituted into core H50S particles only when its sulfhydryl group is free.

Consequently, the potential heavy-atom binding sites on the surfaces of the halophilic ribosomes are being either created by chemical modifications, or inserted by site directed

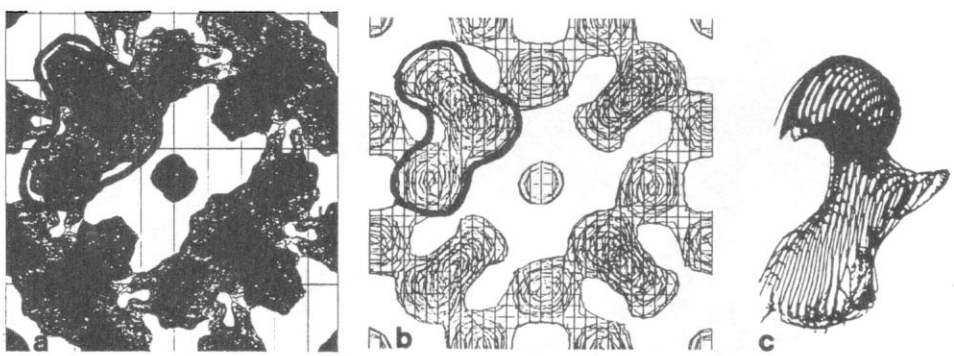

Figure 2: The current preliminary electron density map of T30S.
(a) The MIR map at 19 Å resolution after several cycles of solvent flattening assuming 66% solvent, with final figures of merit of 0.59 and 0.38 for the centric and acentric reflections, respectively. The whole unit cell is shown, down the c axis. The crystals were soaked for 43 and 14 hours in solutions of 3mM of $(NH_4)_6(P_2W_{18}O_{62})14H_2O$ and $(K_5O_2)_3(PW_{12}O_{40})$, respectively. Two major sites were located for the first derivative, and five for the second. The later were partially located in the difference Patterson map and partially in difference Fourier, exploiting the phase information obtained by the first derivative. The combined MIR figure of merit is 0.67. Depicted are the borders of the feature which may be the small ribosomal subunit.
(b) The 40-50 Å map constructed from the amplitude used in (a) and the ab initio phases (50).
(c) The suggested low resolution model for the bound small subunit, based on the subtraction of the large subunit from the model of the whole ribosome (53).

mutagenesis (10, 11). For choosing appropriate locations for these insertions, procedures for specific quantitative detachment and reconstitution of selected ribosomal proteins are being developed, and the surfaces of these ribosomal particles are being mapped by chemical and enzymatic techniques. For the surface mapping experiments as well as for the insertion of the binding sites, sequence information is essential. So far over a third of the ribosomal proteins of *T. thermophilus* (e.g. 12), and more than two thirds of *H. marismortui* have been fully or partially sequenced (Franceschi et al., to be published).

Selective detachment and reconstitution of ribosomal proteins, surface characterization and side chain modifications: Procedures were developed under which six ribosomal proteins (S2, S3, S5, S9, S10 and S14) can be fully detached from T30S (3.4 M LiCl and .5 M urea for 2 hours at 4° C, with gentle agitation, Franceschi et al., to be published). All detached proteins could be reconstituted into the cores lacking them. The reconstituted particles showed 60% of the original poly Phe synthesizing activity.

In parallel experiments, two ribosomal proteins were removed quantitatively by dioxane from H30S. Both detached proteins could be fully reconstituted into the depleted core particles (Franceschi et al, to be published). Using the same procedure, cores of 50S particles, depleted of four proteins, HmaL1, HmaL10, HmaL11 and HmaL12, were prepared. All detached proteins

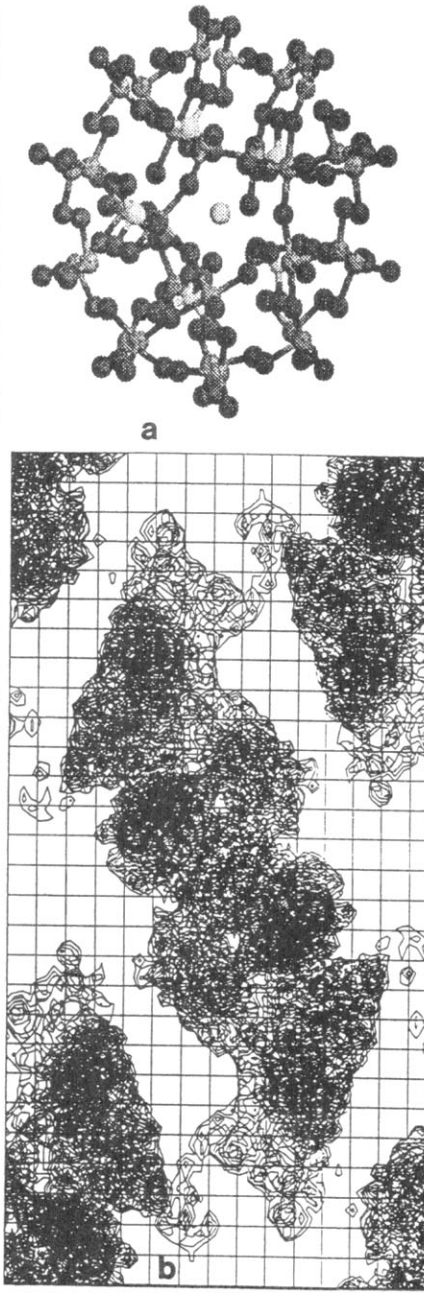

Figure 3:
(a) A schematic view of $K_{14}NaP_5W_{30}O_{110}$, the compound used for initial phasing of the H50S data (constructed from the coordinates given in 54). Dark: O, Medium: W, Light: P. (b) The current MIR map of H50S constructed at 7 Å resolution after several cycles of solvent flattening assuming 60% solvent. A projection of half a unit cell is shown, down the a axis. The crystals were soaked for up to 34 days in solutions containing 1-2 mM of the following clusters: $K_{14}NaP_5W_{30}O_{110}$, $(NH_4)_6(P_2W_{18}O_{62})14H_2O$, $(K_5O_2)_3(PW_{12}O_{40})$ and $Cs_7(P_2W_{17}O_{61}Co(NC_5H_5))nH_2O$. For all sets the Rmerge(I) = 8.4-10.3% and the completeness is 74-91%. Two major sites were located for the first two derivatives, 1 for the third and 4 for the fourth, with occupancies between 0.2 and 0.6). Phasing power between 0.7 (for the $W_{17}Co$ cluster) and 1.36 (for the W_{30} cluster). The overall figure of merit, after two cycles of solvent flattening (assuming 65% solvent) is around 0.65.

can be fully reconstituted and the so obtained particles crystallize under the same conditions as native 50S subunits. However, blocking the -SH group of one of them, HmaL11, prevented its incorporation into the core particles. In this way cores of 50S subunits, depleted of protein HmaL11, were obtained. The ribosomal subunits lacking protein HmaL11 crystallize under the same conditions as the native H50S subunits and at 10 Å show apparent isomorphism with them, indicating that the removal of this protein caused neither major conformational changes in the ribosome, nor gross disturbances in the crystal's network. Therefore it is a suitable candidate for genetic insertions (3, 9).

Surface characterization. An exact definition of the surface of the halophilic ribosomes is currently not possible, as not all the parameters influencing the ribosomal compactness have so far been identified. Nevertheless, several experiments focusing on the exposed regions of the rRNA and the r-proteins, are being carried out.

Probing exposed single stranded rRNA by complementary DNA oligomers gained recently considerable popularity for mapping the ribosome surface (e.g. 13). As the exposed rRNA regions which are involved in functional activity are rather conserved, several such regions have been located on halophilic and thermophilic ribosomes. DNA oligomers, targeting naturally exposed rRNA regions as well as those which become exposed by removing selected ribosomal proteins, have been synthesized. These may be used for derivatization, as they can be prepared with a thiol group at their 5' or 3' ends. The heavy atom clusters may be bound to this end (9).

The targeted regions include the last 14 nucleotides from the 3' end of the 16S RNA (the anti "Shine Dalgarno" region) of T30S and three regions on H50S: bases 1125-1158 of the 23S RNA, homologous to those of *B. stearothermophilus*, which in the wild type are masked by protein BL11 but become exposed in the mutant lacking this protein, bases 1422-1432, the so called "thiostrepton binding site" and bases 2646-2667, the "alfa-sarcin binding site" (reviewed in 11). Among the various undecabase oligomers the tightest hybridization was obtained for the sequence 5'-AAGGAGGTGAT-3', used for complementing the "anti-Shine-Dalgarno" region of the 16S rRNA in T30S. Sucrose gradient centrifugation was performed to purify the hybrid from the unbound oligomers, and the hybridized particles were crystallized. In contrast, for the hybridization of the halophilic "alfa sarcin" region, the salt and magnesium concentrations had to be lowered, suggesting that this site may not be exposed on the surface of the halophilic ribosomes.

Chemical probing of exposed ribosomal proteins. The surface ribosomal proteins are more manageable than the exposed rRNA, therefore they are more suitable for the introduction of specific and quantitative modifications. Earlier accessibility studies were concentrated on limited proteolysis under conditions optimized for *E. coli* (14). Attempts to extend the proteolytic experiments to the halophilic ribosomes were only partially successful, because the halophilic ribosomes require high salinity for maintaining their compactness, whereas the conditions suitable for the proteolytic reaction of all the commercially available enzymes are milder. Therefore, even when using the most robust proteolytic mixtures, partial unfolding of the halophilic ribosomes could have occurred. Such unfolding may not effect dramatically the overall sedimentation coefficient, showing that the gross

integrity of the ribosomes is being kept, but at the same time, an opening-up of the compact active conformation and consequently exposing internal residues cannot be ruled out. An alternative procedure is to decorate the surface of the ribosomes by chemical means. Our attempts at probing the exposed cysteines have been reported (3, 9, 15, 16). The exposed amino groups, N-terminals and lysines' side chains, were probed by mild methylation, extending the procedures reported by (17) and acylation with various radioactive agents. As expected, only in a few occasions these modifications reached completeness. In typical experiments 30-60% of the lysines of H50S became modified, depending on the experimental conditions. It remains to be seen if the rest of the lysines are engaged in internal contacts. Interestingly, the H50S particles which were exposed to a rather low methylation levels (25% of the original amount) yielded crystals, which on several occasions reached an unusual large size (11).

The modified proteins were detached from the particle, digested with the endoproteinase Lys-C, and the resulting peptides were analyzed for labeled lysines. So far several exposed regions have been identified on HmaL1 and HmaL12 (S. Weinstein and M. Peretz, to be published).

H30S subunits behave differently and undergo substantial disintegration upon methylation, in accord with the lower stability and higher sensitivity found for several small eubacterial ribosomal subunits by different methods (18, 19). In contrast, T30S was readily methylated to completion while maintaining its integrity.

Site directed mutagenesis: The surface mapping experiments were synchronized with the characterization of the genes coding for the surface proteins which can be detached and reincorporated into core particles lacking them. Furthermore, these proteins were overproduced in *E. coli*, using the pET expression system (20). Despite the relatively low intracellular salt concentration of *E. coli*, the halophilic overproduced proteins reached the level of 30-40% of the total cell proteins and remain soluble in the cytoplasm. Unexpected complications were encountered in attempts at amplifying by PCR HmaL12 and the HmaL12/HmaL10 gene complex, presumably because of unusual stable folding of this gene region. These were overcome by the design of the appropriate oligonucleotide primers according to the thermodynamic algorithm (21).

As all overproduced proteins can be incorporated into cores lacking them, giving rise to active ribosomal particles (11), the way to site directed mutagenesis became open. PCR (22) or the procedures described by (23) were used for site directed mutagenesis. So far seven different mutants of HmaL1 and ten of HmaL11 have been engineered, in each case, a cysteine codon was inserted on different regions of the protein. To avoid undesired binding, the natural cysteine of HmaL11 was exchanged by a serine, as it was found to be unsuitable for labeling (see above, and 9).

The production of core particles, depleted of protein HmaL11 (see above), simplified the analysis of the incorporation of the mutated protein HmaL11. With the exception of two mutants, all could be incorporated into core particles. Screening for the suitability of the mutated proteins for binding heavy atom clusters, is in progress. The differences in the ability of the various mutated proteins to incorporate into the depleted cores may provide

indications about the conformation of the ribosomal proteins and/or their specific in-situ interactions. These are being currently analyzed.

The Isolation and Characterization of in situ Complexes

The knowledge of the accurate molecular structures of ribosomal components should provide a powerful tool for higher resolution structure determination of the entire particle. It is anticipated to benefit from the crystallographic analysis of isolated r-proteins eg. S5(24), S6 (25), L1(26), L6 (27), L9 (28) L7/12 and L30 (29), although it remains to be seen whether their structures reflect their in-situ conformations. Extending these studies to the large halophilic ribosomal subunit, internal small and defined sub-structures of them have been chosen, since it is more likely that these maintain their native conformation, as they may conserve their in situ micro environment. During the course of the surface mapping and depletion studies on H50S, two in situ stable complexes have been identified. The first is between protein HmaL1 and a stretch of about 120 nucleotides of 23S rRNA, which was characterized mainly by limited digestion, the second is between two proteins: HmaL10 and HmaL12.

The experimental procedures and the biochemical properties of the ribonucleoprotein complex have been described (30). Interestingly, despite the "exotic" properties of the halophilic ribosomes, and the evolutionary distance between *Haloarcula* and *E. coli*, both archaebacterial components of this complex are readily interchangeable with their eubacterial counterparts (30).

The existence of a complex between proteins HmaL10 and HmaL12 was revealed by the comparison of the two-dimensional gels of the total proteins of H50s and those belonging the group which is detached by dioxane. It was shown that proteins HmaL10 and HmaL12 move together even at 8M urea, indicating the existence of a stable complex between them. This complex dissociates into two separate proteins by dioxane and perhaps also in SDS. Although still no fully analyzed in quantitative terms, namely, whether it contains one or four copies of protein L12, as found for eubacteria (reviewed in 31), eukaryotes (32) and other archaebacteria (33), it is clear that this is a remarkably stable complex which does not disintegrate at 8 M urea or the FPLC conditions. Therefore it is expected to form ordered crystals, of a higher quality than those of its homologue from *B. stearothermophilus* (34).

As all components of these complexes have been overexpressed, they are being produced in amounts sufficient for their crystallization as well as for their derivatization and incorporation in core particles. In addition, all three proteins participating in these complexes can be detached from H50S by dioxane, indicating that they are located at the surface of the particle, thus providing potential cluster binding sites. In case these complexes will yield a high resolution structures, the combination of their structure with the expected localization of the clusters bound to them in the electron density map of the particle should be most important for further map interpretation.

Utilizing the Ribosomal Models Reconstructed From Crystalline Monolayers For Further Structural and Functional Studies

Images of the 70S ribosome and its large subunit from *B. stearothermophilus* were recon-

structed at 47 and 28 Å respectively, using tilt series of crystalline arrays, negatively stained with an inert material (35; 36). Although image reconstruction is not free from experimental and conceptual limitations, its superiority over conventional electron microscopy methods was demonstrated by the exclusive detection of several key features, associated mainly with internal vacant or partially filled hollows. Hence, despite their low resolution, the reconstructed models were provisionally interpreted (18). Consequently, it was suggested that the biosynthetic reaction occurs at the intersubunit interface, and plausible locations for the sheltered paths of the nascent proteins and of the mRNA chains were identified (18, 37).

The reconstructed models inspired the design and the crystallization of complexes of ribosomal particles, mimicking defined functional states. These include 50S subunits to which one tRNA molecule and a short polypeptide are bound (38) and 70S ribosomes with a short stretch of mRNA and two molecules of tRNA (39). The superiority of the later over crystals of 70S ribosomes is evident. All three-dimensional crystals of 70S obtained so far are either too small or diffract to a very low resolution, 20-45 Å, presumably due to their significant conformational heterogeneity. In contrast, even the very simple complex, composed of 70S ribosome, two phetRNA^{phe} molecules and a chain of about 35 uridyl residues (as messenger RNA), led to a dramatic improvement in the reproducibility of crystal growth and to an increase of over 10 Å in the resolution limits (39).

More sophisticated complexes of T70S have recently been designed, aimed at increasing the homogeneity of the functional complexes of T70S and at minimizing the chances of protruding stretches of mRNA. These contain around 18 nucleotides, as this is the approximate length of mRNA on both sides of the decoding site, which is masked by the ribosome (40). Best results were obtained for $(ATC)_5$-CTT. Including in the reaction mixture charged tRNA^{ile} and omitting tRNA^{leu}, crystals of the complex with an average of 1.6 molecules of leu-tRNA^{ile} have been obtained.

Since tRNA participates in all so far crystallized complexes of ribosomal particles, trapped at defined functional states, a procedure was designed for the specific labeling of tRNA^{phe} and tRNA^{ile} by reagents made of multi-metal clusters, in a fashion which does not hamper the aminoacylation by the corresponding synthetase and the binding to the ribosome (16). The complexes containing the gold-cluster bound tRNA molecules were crystallized and are being exposed to crystallographic analysis.

The provisional interpretation of the reconstructed models stimulated also various biochemical experiments, which, in turn, provided the basis for computed modeling, attempting at shedding light on the progression of the growing polypeptide chains (41, 42). Of particular interest is the fate of the MS2 coat protein. Biochemical studies indicated that the labeled N-terminal of this protein is not available for interaction with antibodies raised against the label, until the protein reaches its full length, 129 amino acid residues. Indeed, the modeling experiments showed that the entire protein can be accommodated in a partially folded conformation within the tunnel which span the 50S subunit, assumed to be the path of the nascent chains. These studies accord with results of activation-release studies, showing that the final steps in the folding of nascent proteins are mediated by chap-

erons associated with the ribosome (40, 42, 43, 44).

It is clear that a higher resolution is essential for more accurate assignments. Therefore image reconstruction experiments from unstained crystalline arrays in vitrified ice are being carried out. Preliminary efforts led to the growth of arrays of 50S subunits, diffracting to about 15 Å resolution (45).

First Steps in Isomorphous Replacement Phasing Using Soaked Crystals

The derivatization of macromolecular crystals may be performed in two ways: either by covalent specific binding of the heavy atom prior to crystallization, an example for which was given above, or by soaking crystals in solutions containing the heavy atoms. The latter is more common, since the experimental requirements are rather simple and the results can be assessed in a relatively short time. Using this trial-and-error procedure, productive single-site derivatization is largely a matter of chance. However, the probabilities of successful derivatization are sufficiently high that more sophisticated techniques are rarely needed.

A thorough search for potential suitable compounds and parameters for soaking the ribosomal crystals has been performed, concentrating on the clusters and coordination compounds listed in TABLE I. As mentioned above, these compounds were chosen because their densities were calculated to be sufficient for phasing structures of sizes of the order magnitude of those of the ribosomal particles, providing high occupancies.

1. Preliminary phasing at 17-19 Å resolution of X-ray data of T30S

Soaking crystals of T30S (2) in solutions containing the heteropolyanion $(NH_4)_6(P_2W_{18}O_{62}).14H_2O)$ (46) or $(K_5O_2)_3(PW_{12}O_{40})$ (47), led to preliminary phasing at 15 Å resolution. A third derivative, Ta_6Br_{14}, which proved to be useful for structure determination of large assemblies and proteins (48, 49), is currently being investigated.

Initially the two W derivatives were phased independently, using only the centric reflection for the construction of two SIR maps at around 20 Å resolution. No attempt was made to resolve the individual atoms of the heteropolyanions. These were treated as group scatterers. The 12 W atoms cluster was approximated to a sphere, whereas the 18 W atoms cluster, which has an ellipsoidal shape and is actually composed of two 9 W atoms clusters, was represented by two 9 W scatterers. The figures of merits of these maps are 0.57 for 240 centric reflections (phasing power 1.78) 0.44 for 270 centric reflections (phasing power 1.02).

Combining the phase information from both derivatives yielded a not interpretable 19 Å MIR electron density map. However, after several cycles of solvent flattening combined with density modification, the resulting electron density map (Fig. 2) contains features which may be interpreted as small ribosomal particles, and its packing motif is in accord with that observed in thin sections of embedded crystals (Fig. 2). Furthermore, this map shows striking agreement with that constructed from independent phase information (Fig. 2) obtained by the maximum entropy combined by likelihood ranking approach (50).
Despite the reasonable quality of the crystallographic parameters of the preliminary MIR

map, the borders of the individual particles are still not clear. Attempts towards this aim are currently being carried out by subjecting the current phases to extension procedures, aiming at considerably higher resolution, 12-14 Å. Once the envelop of this particle is determined, it will be compared to both the commonly observed views of free small subunit, obtained by traditional and sophisticated electron microscopy (for review see 51,52), and to that of the bound small subunit, resulting from the subtraction of the model of the large subunit from that of the whole ribosomes (Fig. 2 and in 53).

2. Preliminary phasing at 7 Å resolution of X-ray data of H50S

Preliminary partial phase information was obtained for the crystals of H50S (1) by soaking crystals in solutions of $K_{14}NaP_5W_{30}O_{110}$ (54), $(NH_4)_6(P_2W_{18}O_{62})14H_2O$ (46), $(K_5O_2)_3(PW_{12}O_{40})$ (47) and $Cs_7[P_2W_{17}O_{61}Co(NC_5H_5)]nH_2O$ (M. Pope, private communication). Although the resolution of the soaked crystals was lower than that of the native ones (2.9 Å), all derivatives diffracted well beyond 7 Å, and in many cases, well shaped reflections were detected at 3.5-5 Å. However, because of technical reasons and synchrotron beam-time limitations, data were collected only to lower resolution. The initial difference Patterson map was constructed at 12 Å resolution, using the data collected from a crystal soaked in $K_{14}NaP_5W_{30}O_{110}$. Significant sophistication was required for the interpretation of the difference Patterson maps, including partial assignment of the individual atoms. Nevertheless, the sites detected in the difference Patterson map were reconfirmed by ab-initio calculations (see below).

These phases were used for the construction of the difference electron density maps between the native and the other three derivatives, which revealed that all four clusters occupy roughly the same site. Therefore their phase information was used mainly for extending the resolution of the initial map. The connectivity within the map was significantly enhanced when the lower resolution reflections were included, and it was subjected to two cycles of solvent flattening, assuming that the crystals contain 65% solvent (Fig. 3).

Complementary Studies: Low Resolution Phasing By Computational and Semi Experimental Methods

In small molecule crystallography phases are routinely obtained by ab-initio methods (55). The elegance of these methods stimulated a considerable effort for their extension towards macromolecules. Consequently, a large range of approaches is being exploited in the context of low-resolution phasing of the ribosomal reflections.

Entropy maximization with log likelihood gain as a phase-set discriminator (56) was used to suggest the packing and to detect some envelop features of T50S at a resolution of about 80 Å (57, 58). These results were later supported by the application of the few atom method (59) and by low-resolution molecular replacement studies (60), using the approximate model reconstructed for this particle (36). Molecular replacement studies with this model have also been performed on other crystal forms (53, 61).

Furthermore, the positioning of the center of mass of T50S was supported by results of

ultra-low resolution R-factor searches at various solvent contrasts (57, 62) and by the application of an extension of traditional direct methods combined with ellipsoidal modeling (63, 64). A visual summary of these efforts is given in Fig. 4.

A new approach, combining elements of traditional direct methods, envelop refinement, maximum entropy filtering, likelihood ranking, cross validation and cluster analysis, aiming at phasing at resolution up to 30 Å (Volkmann, to be published), has been applied to T50S and led to results that agree well with the previous ones (50). The same approach was applied to data from H50S crystals, and the resulting weights and phases were used to locate heavy atom sites by difference Fourier calculations (N. Volkmann and H.A.S. Hansen, to be published), which were found to be the same as determined by difference Patterson interpretation (see below).

Direct information about packing motifs of the ribosomal crystals has been derived by electron microscopy since the large size of the ribosome enables its observation. In these experiments three-dimensional crystals are being embedded in epon and sectioned at preferred orientations to extremely thin slices, of a thickness similar to one unit cell. Optical diffraction information, obtained from their electron-micrographs, together with visual inspection and symmetry considerations, can be exploited to yield information about the packing arrangements of the crystals. This information was combined with the results of real and reciprocal space searches and led to the determination of the number of the ribosomal particles in the asymmetric unit (see below and in 5).

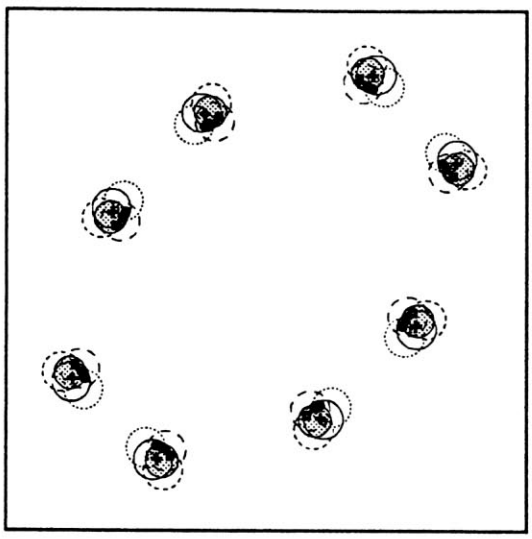

Figure 4: The positions of the centroids of electron density maps derived by various methods for X-ray data collected from native and gold thioglucose (GTG) soaked crystals of the large ribosomal subunit of *Thermus thermophilus*. The size of the circles is given by the estimated root mean square of the corresponding position if an estimated was available. The plot corresponds to a z-projection of the whole unit cell.

Conclusions and Prospects

From the early stages of ribosomal crystallography, it was clear that a straight-forward application of conventional concepts and techniques of macromolecular crystallography would not be adequate. Hence we designed an approach which combines the exploitation of the extensive information available on the genetic, functional and chemical properties of ribosomes for a rational design of protocols for crystallization and for

derivatization with dense clusters or multi-atom salts. As seen, preliminary maps at intermediate resolution which show features of the size expected for the corresponding ribosomal particles, have already been constructed. Furthermore, since the native and several derivatized crystals diffract to relatively high resolution, up to 2.9 Å for H50S and 7.3 for T30S, a more detailed map is anticipated in the foreseeable future.

Acknowledgements

The studies presented here have been initiated under the inspiration and guidance of the late Prof. H.G. Wittmann. We are grateful to the excellent experimental assistance provides by Mr. K. Knaak and T. Arad as well as Ms. C. Glotz, R. Albrecht, C. Paulke, J. Müssig, J. Piefke, R. Hasenbank, B. Romberg, I. Dunkel, B. Schroeter, S. Meyer, C. Radzwil, B. Donzelmann, M. Laschever and P. Baruch. We thank Drs. M. Pope, W. Jahn, R. Huber, W. Bode and W. Preetz for their gifts of multi-metal compounds and Dr. F. Triana for the preparation of tRNA molecules. We also thank Drs. M. Roth, E. Pebay-Peyroula, B. Hardesty, A. Podjarny, W. Hill, E. Dabbs, K.R. Leonard and W. Chiu for their active participation in the studies presented here and for their illuminating comments.

This work was carried out at the Max-Planck-Institute for Molecular Genetics in Berlin, the Max-Planck-Research-Unit at DESY in Hamburg, the Weizmann Institute of Science, and the following synchrotron facilities: EMBL and MPG beam lines at DESY, Hamburg; CHESS, Cornell University; SSRL, Stanford University; and PF/KEK, Japan. Support was provided by the National Institute of Health (NIH GM 34360), the German Federal Ministry for Research and technology (BMFT 05 180 MP BO), the German space agency DARA (50QV 86061), the Minerva Fellowship Program and the Kimmelman Center for Macromolecular Assembly at the Weizmann Institute. AY holds the Martin S. Kimmel Professorial Chair.

References and Footnotes

1. von Böhlen K., Makowski I., Hansen H.A.S., Bartels H., Berkovitch- Yellin Z., Zaytzev- Bashan A., Meyer S., Paulke C., Franceschi F. and Yonath A. *J. Mol. Biol., 222*, 11-15 (1991).
2. Yonath, A., Glotz, C., Gewitz, H.S., Bartels, K., von Böhlen, K., Makowski, I., and Wittmann, H.G. *J. Mol. Biol. 203*, 831-4 (1988).
3. Berkovitch-Yellin, Z., W.S. Bennett and A. Yonath. *Critical Reviews in Biochemistry and Molecular Biology 27*, 403-439 (1992).
4. Jahn, W. *Z. Naturforsch. 44b*, 1313-1316 (1989).
5. Bartels, H., Bennett, W.S., Hansen, H.A.S., Eisenstein, M., Weinstein, S., Müssig, J., Volkmann, N., Schlünzen, F., Agmon, I., Franceschi, F. and Yonath, A. *J. Peptide sciences*, in the press (1995).
6. Müssig J., Makowski I., von Böhlen K., Hansen H., Bartels K.S., Wittmann H.G. and Yonath A. *J. Mol Biol. 205*, 619-22 (1989).
7. Schlünzen, F., Hansen, H.A.S., Thygesen, J., Bennett, W.S., Volkmann, N., Levin, I., Harms, J., Bartels H., Zaytzev-Bashan, A., Berkovitch-Yellin, Z., Sagi, I., Franceschi, F., Krumbholz, S., Geva, N., Weinstein, S., Agmon, I., Böddeker, N., Morlang, S., Sharon, R., Dribin, A., Maltz, E., Peretz, M., Weinrich, V., and Yonath, A. In: *Frontiers in Translation* Ed. A. Matheson et al. special issue of Biochemistry and Cell Biology, in the press (1995).
8. Jahn, W. *Z. Naturforsch. 44b*, 79-82 (1989).
9. Franceschi F., Weinstein S., Evers U., Arndt E., Jahn W., Hansen H.A.S., von Böhlen K., Berkovitch-Yellin Z., Eisenstein M., Agmon I., Thygesen J., Volkmann N., Bartels H., Schlünzen F., Zaytzev-Bashan A., Sharon R., Levin I., Dribin A., Sagi I., Choli- Papadopoulou T., Tsiboli P., Kryger G., Bennett W.S. and Yonath A. In: *The Translational Apparatus*, edited by K. Nierhaus, F. Franceschi, A. Subramanian, V. Erdmann and B. Wittmann-Liebold, Plenum Press. pp. 397-410 (1993).

10. Franceschi F., Sagi I., Böddeker N., Evers U., Arndt E., Paulke C., Hasenbank R., Laschever M., Glotz C., Piefke J., Müssig J., Weinstein S., and Yonath A. 1994. In: *Molecular Biology of Archaea* Edited by F. Pfeifer, P. Palm and K.H. Schleifer. Gustav Fischer Verlag, pp. 197-205 (1994).
11. Sagi I., Weinrich V., Levin I., Glotz C., Laschever M., Melamud M., Franceschi F., Weinstein S. and Yonath A. *Biophys J.* in the press (1995).
12. Tsiboli, P., Herfurth, E. and Choli, T. *European J. of Biochem. 226*, 169-77 (1994).
13. Weller, J. and Hill, W.E. *Biochemie 73*, 971-81 (1991).
14. Kruft V. and Wittmann-Liebold B. *Biochemistry 30*, 11781-7 (1991).
15. Weinstein, S., Jahn, W., Wittmann H.G. and Yonath, A. *J. Biol. Chem., 264*, 19138-42 (1989).
16. Weinstein, S., Jahn, W. Laschever, M., Arad, T. Tichelaar, W., Haider, M., Glotz, C., Boeckh,T., Berkovitch-Yellin, Z., Franceschi, F. and Yonath, A. *J. Crys. Growth, 122*, 286-92 (1992).
17. Rayment, I., Wojciech, R., Rypniewski, Schmidt-Base, K., Smith, R., Tomchick, D.R., Benning, M.M., Winkelmann, D.A., Wesnberg, G. and Holden, H.M. *Science 261*, 50-53 (1993).
18. Yonath A. and Wittmann, H.G. *TIBS 14*, 329-34 (1989).
19. Evers U., Gewitz H.S. 1989. *Biochem. Internat. 19*, 1031-8 (1989).
20. Studier, F.W., Rosenberg, A.H., Dunn, J.J. and Dubendorf, J.W. *Meth. in Enzymol. 185*, 60- 88 (1990).
21. Rychlik W. and Rhoads R. *Nucleic Acids Research 17*, 8543-51 (1989).
22. Picard, V., Edsal-Badju, E., Lu, A. and Book, S.C. *Nucleic Acid Research 22*, 2587-91 (1994).
23. Sayers, J.R., Krekel C. and Eckstein, F. *Biotechniques 13*, 592-6 (1992).
24. Ramakrishnan, V. and White, S.W. *Nature 358*, 768-71 (1992) .
25. Lindahl, M., Svensson, L.A., Liljas, A., Sedelnikova, S.E., Eliseikina, I.A., Fomenkova, N.P., Nevskaya, N., Nikonov, S.V., Garber, M.B., Muranova, T.A. et al. *EMBO J. 13*, 1249-54, (1994)
26. Nikonov, S., Nevskaya, N., Eliseikina, I., Fomenkova, N., Nikulin, A., Garber, M, Aevarsson, Svensson, A.L., Al-Karadaghi, S. Briand, C., Unge, J. and Liljas A. In: *Frontiers in Translation* Ed. A. Matheson et al. special issue of Biochemistry and Cell Biology, in the press (1995).
27. Golden B., Ramakrishnan V., and White SW. *EMBO J. 12*, 4901-8 (1993).
28. Hoffman, D.W., Davies, C., Gerchman, S.E., Kycia, J.H., Porter, S.J., White, S.W. and Ramakrishnan V. *EMBO J. 13*, 205-12 (1994).
29. Leijonmarck, M., Appelt, K., Badger, J., Liljas, A., Wilson, K.S. and White S.W. *Proteins 3*, 243-251. (1988).
30. Evers, U., F. Franceschi, N. Boeddeker and A. Yonath. 1994. *Bioph. Chem. 50*, 3-16 (1994).
31. Moller, W. and Maasen, J.A. In: *Structure, Function and Genetics of Ribosomes*, Edited by B. Hardesty and Kramer G., Springer Verlag, NY, pp. 309-25 (1986).
32. Saenz-Robles, M.T., Villela, M.D., Pucciarelli, G., Polo, F., Remacha, M., Ortiz, B.L., Vidales, F.J. and Ballesta, J.P.G. *Eur. J. Biochem. 177*, 531-7 (1988).
33. Casiano, C. Matheson, A.T. and Traut, R.R. *J. Biol. Chem. 265*, 18757-61. (1990).
34. Liljas A., and Newcomer M.E. *J. Mol. Biol. 153*, 393-8 (1981).
35. Arad, T., Piefke, J., Weinstein, S., Gewitz, H.S., Yonath, A. and Wittmann H.G. *Biochimie, 69*, 1001-1006 (1987)
36. Yonath, A., Leonard, K.R. and Wittmann, H.G. *Science 236*, 813-7 (1987).
37. Yonath A. and Berkovitch-Yellin Z. *Current Opinion in Structural Biology 3*, 175-81 (1993).
38. Gewitz, H.S. Glotz, C. Piefke, J. Yonath, A. & Wittmann, H.G. *Biochimie, 70*, 645-8 (1988).
39. Hansen, H.A.S., N.Volkmann, J.Piefke, C.Glotz, S.Weinstein, I. Makowski, S.Meyer, H.G.Wittmann & A.Yonath. *Biochem. Biophys. Acta 1050*, 1-7 (1990).
40. Beyer, D., Skripkin, E., Wadzack, J. and Nierhaus, K.H. *J. Biol. Chem. 269*, 30713-7 (1994).
41. Eisenstein M., Hardesty B., Odom M., Kudlicki W., Kramer G., Arad T., Franceschi F. & Yonath A. In: *Supramolecular Structure* (G. Pifat Ed.) Balaban Press, Rehovot, pp. 213-246 (1994).
42. Hardesty B., Yonath A., Kramer G., Odom O.W., Eisenstein M., Franceschi F. and Kudlicki W. In: *Membrane Protein Transport* (S.S. Rothman, Ed.), in the press (1995).
43. Kudlicki, W., Odom, O.W., Kramer, G. and Hardesty, B. *J. Biol. Chem. 269*, 16549-53 (1994).
44. Kudlicki, W., Odom, O.W., Kramer, G. and Hardesty, B. *J. Mol. Biol. 244*, 319-31 (1994).
45. Avila-Sakar A.J., Guan T.L., Schmid M.F., Loke T.L., Arad T., Yonath A., Piefke J., Franceschi F. and Chiu W. *J. Mol. Biol. 239*, 689-697 (1994)
46. Dawson B., *Acta Crystallography. 113*, 2953-6 (1953).
47. Brown, G.M., Noe Spirlet, M.R., Busig W.R. and Levy, H.A. *Acta Crys. B33*, 1038-1046 (1977).
48. Schneider, G. and Lindquist, Y. *Acta Cryst. D50*, 186-191 (1994).
49. Löwe J., Stock D., Jap B., Zwickl P., Baumeister, W. and Huber, R. *Science, 268*, 533-9. (1995).
50. Volkmann, N. Schlünzen, F., Vernoslava, E.A., Urzhumstev, A.G., Podjarny, A.D., Roth M.

and Pebay-Peyroula E., Berkovitch-Yellin, Z., Zaytzev-Bashan, A. and Yonath, A. *Joint CCP4 and ESF-EACBM Newsletters*, in the press (1995).
51. *The Translational Apparatus*, edited by K. Nierhaus, F. Franceschi, A. Subramanian, V. Erdmann and B. Wittmann-Liebold, Plenum Press.(1993).
52. *The Ribosomes: Structure, Function and Evolution*, Edited by Hill, E.W., Dahlbert, A. Garrett, R.A., Moore, P.B., Schlesinger, D. and Warner, J.R., American Society for Microbiology, Washington, D.C., (1990).
53. Berkovitch-Yellin, Z., Wittmann, H.G. and Yonath, A. *Acta Crystallography B46*, 637-42 (1990).
54. Alizadeh M.H., Harmalker, S.P., Jeannin Y., Martin-Frere J. and Pope M.T. *J. Am. Chem. Soc. 107*, 2662-2669 (1985).
55. Giacovazzo, C. *Direct Methods in Crystallography*, Academic Press, London. (1980).
56. Bricogne, G. *Acta Crys. A40*, 410-445 (1984).
57. Volkmann N. Ph. D. Thesis. Maximum entropy and the phase problem for ribosomal crystallography. University of Hamburg, Germany (1993).
58. Volkmann N. In: *Entropy, Likelihood, Baysian Inference and their Application in Crystal Structure Determination*, Edited by G. Bricogne, American Cryst. Assoc. in the press (1995).
59. Lunin, V.Y., Lunina, N.M., Petrova, T.E., Vernoslava, E.A., Urzhumstev, A.G. and Podjarny, A.D. *Acta Cryst. D51*. in the press. (1995).
60. Urzhumstev, A.G. and Podjarny, A.D. *Acta Cryst. D51*. in the press (1995)
61. Eisenstein M., Sharon R., Berkovitch-Yellin Z., Gewitz H.S., Weinstein S., Pebay-Peyroula E., Roth M. and Yonath A. *Biochemie 73*, 879-886 (1991).
62. Schlünzen F. Crystallographic investigations on the 50S ribosomal subunits from Thermus thermophilus. Ph.D. Thesis, U. of Hamburg, Germany (1994).
63. Roth M. and Pebay-Peyroula E. 1995. In: *Entropy, Likelihood, Baysian Inference and their Application in Crystal Structure Determination*, Edited by G. Bricogne, American Cryst. Assoc. in the press (1995).
64. Zaytzev-Bashan A. Ph.D. Thesis. Crystallographic studies on the large ribosomal subunits from halophilic and thermophilic bacteria. Weizmann Inst. Rehovot, Israel (1995).
65. Bartels, H. Crystallographic investigations on the large ribosomal subunit from Bacillus stearother mophilus. Ph.D. thesis, Frei Universität Berlin, Germany (1995)